Space Charge Effects in Fourier Transform Mass Spectrometry. Mass Calibration

Edward B. Ledford, Jr., Don L. Rempel, and M. L. Gross*

Department of Chemistry, University of Nebraska, Lincoln, Nebraska 68588

A new relationship between ion mass and effective cyclotron frequency is derived for ions stored in a cubic cell and detected by using Fourier transform mass spectrometry. An assessment of collisional damping on mass measurement error is also made. It is concluded that frequency perturbation by collisional damping, while predicted by the model, is negligible at sufficiently low pressure. The mass calibration law is tested at a magnetic field of 1.2 T by using major fragment ions of 1,1,1,2-tetrachloroethane. With broad band "chirp" excitation of ions, systematic rather than random errors were discovered. The magnitude of these systematic errors increased as the number of ions stored in the cell was increased. However, it is predicted from the calibration law that errors will decrease with the square of the magnetic field strength.

The Fourier transform mass spectrometer (FTMS) (*1*) is recognized as a potentially useful analytical instrument because it is capable of high mass range and ultrahigh mass resolution. The demonstration of high resolving power with the FTMS, however, has predated by several years the development of methodology for exact mass measurement and elemental composition assignment.

Early attempts to produce a mass calibration scheme sufficiently accurate for elemental composition assignments were not successful. For example, Ledford and McIver (*2*) reported measurement accuracy ranging from 7 ppm to 151 ppm over the mass range m/z 47 to m/z 264 using an ICR mass spectrometer with electrometer detection. The mass errors were systematic, caused by changes in space charge conditions in the analyzer cell as ions were sequentially observed. Comisarow (*3*) reported mass measurement accuracy ranging from 0.3 ppm to 80 ppm over the mass range m/z 69 to m/z 1166. The relative measurement errors were found to increase systematically with mass.

Mass measurement accuracy of the a few parts per million or less (often sufficient for elemental composition assignment) was achieved in more recent studies. Ledford (*4*) et al. investigated mass measurement using a parabolic mass calibration law for cubic analyzer cells. Over a 4 amu mass range, errors of 0.8 ppm were typical, while average errors of 2 ppm over an 18 amu mass range were obtained when a three-parameter fit was used. Wanczek and Allemann (*5*) reported a novel side-band method for measuring the masses of trapped ions. Errors averaging 1.5 ppm were obtained over the mass range m/z 18 to m/z 170 amu.

Although these latter methods (*4*, *5*) of calibration represent improvements over earlier work (*2*, *3*), they have not proved to be routinely useful for exact mass determination. One reason is that ion space charge in the analyzer cell affects observed frequencies, and this must be accounted for in accurate measurements. Ledford et al. (*4*) recognized this in their efforts to develop a mass calibration scheme. They demonstrated that frequency shifts associated with changes in space charge were qualitatively similar to those caused by changes in trap voltage. White et al. (*6*) have attempted to compensate for space charge induced frequency shifts. They found that correct elemental compositions could be assigned in the absence of reference ions provided the instrument was calibrated under space charge conditions nearly identical with those of the original exact mass measurements.

Recently, Jeffries et al. (*7*) have advanced a theory of space charge induced frequency shifts in Penning cells of various geometries. This theory is based on the premise that a thermal ion ensemble assumes the form of an ellipsoid of uniform charge density. From the theory, one may conclude that small changes in space charge density mimic small changes in trap voltage, and this is in accord with empirical observations (*4*). Francl et al. (*8*) have derived from this theory an approximate mass calibration procedure and have tested this procedure in a limited way.

In this paper we show that the calibration procedure of Francl et al. (*8*) may be applicable only over narrow mass ranges because of the approximations made in the derivation. An alternative mass calibration procedure has been derived, without using approximations, and tested under realistic circumstances where space charge effects become detectable, i.e., in the range of 10 000 to 100 000 ions in the analyzer cell.

THEORY

Approximate Mass Calibration. Jeffries et al. have derived the following expression for the frequencies of the natural modes of single ion motion in a cubic Penning cell (ref 7, eq 31):

$$\omega_{\pm} = (\omega_c/2)\{1 \pm [1-4(2qV_TG_T/m + \rho q^2G_i/\epsilon_0 m)/\omega_c^2]^{1/2}\} \quad (1)$$

For this discussion, the salient parameters are ω_+, the angular frequency of the cyclotron mode, B, the magnetic field strength, V_T, the trap voltage, ρ, the charge density, m, the mass of the ion, and ω_c the cyclotron frequency, which is given by

$$\omega_c = qB/m \quad (2)$$

An approximate mass calibration procedure has been derived by linearizing eq 1 about the point $m = 0$, $V_T = 0$, and $\rho = 0$ to yield (ref 8, eq 7)

$$\omega_{eff} = \omega_c - 2\alpha V_T/a^2B - q\rho G_i/\epsilon_0 B \quad (3)$$

There follows (ref 8, eq 8)

$$\omega'_{eff} - \omega''_{eff} = qB(1/m' - 1/m'') \quad (4)$$

for any two masses in a given spectrum. If B is known, the charge to mass ratio q/m' of an unknown can be determined relative to a reference ion of q/m'' by measuring the frequency difference $\omega'_{eff} - \omega''_{eff}$. Francl et al. (*8*) reported a mass measurement accuracy of 0.8 ppm for an ion of nominal mass m/z 156 relative to a calibrant ion at m/z 157.9549. While this result is encouraging, the error associated with the linearization and the consequences for the the general use of the approximate mass calibration procedure were not discussed except to note that the approximation errors were about 0.3

0003-2700/84/0356-2744$01.50/0

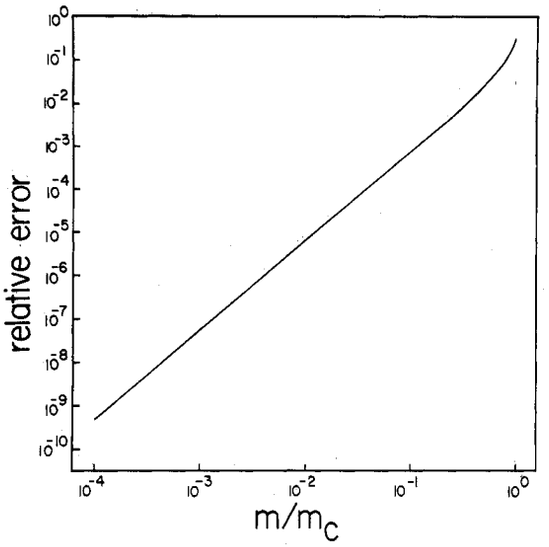

Figure 1. Variation of theoretical relative error (ϵ) with the ratio m/m_c where m is the ion mass and m_c is the critical ion mass.

ppm for the conditions of their experiment and that the approximation errors would become smaller at higher magnetic field strength.

Error Analysis. To facilitate the discussion of the error made in eq 3 by the linearization of eq 1, we shall make some definitions. Put

$$V_{T'} \triangleq \rho(qG_i/2\epsilon_0 G_T) \tag{5}$$

$$V_{eff} \triangleq V_T + V_{T'} \tag{6}$$

$$m_c/q \triangleq B^2/8V_{eff}G_T \tag{7}$$

Then eq 1 becomes

$$\omega_\pm = (\omega_c/2)\{1 \pm [1 - m/m_c]^{1/2}\} \tag{8}$$

Using (ref 7, Table I)

$$G_T = \alpha/a^2 \tag{9}$$

together with the above definitions, eq 3 becomes

$$\omega_{eff} = (\omega_c/2)\{2 - (1/2)(m/m_c)\} \tag{10}$$

The relative error of the linearization is evaluated as

$$\epsilon = (\omega_{eff} - \omega_+)/\omega_+ \qquad 0 \le m/m_c \le 1 \tag{11}$$

For exact mass measurements, where errors are expected to be in the low parts-per-million range, it is not desirable to make approximations which introduce errors of more than 0.1 ppm. A plot of relative error ϵ vs. m/m_c (Figure 1) shows that to avoid errors greater than 0.1 ppm through use of eq 3, the ratio m/m_c must be restricted to a value ≤ 0.0013. We will now examine the implications of this.

Critical Mass. Definition 7 is significant because, for $m/q \ge m_c/q$, the discriminant in eq 8 vanishes or changes sign. Physically, ion motion becomes unstable. The magnetic force can no longer overcome the electric force, and radial confinement of the ions is no longer possible (*9*, *10*). Thus, a fundamental upper bound on the mass range of an FTMS or ICR experiment is m_c/q. For conditions similar to those used in this study, $B = 1.2$ T, $V_{eff} = 1$ V, $a = 0.0254$ m, $\alpha = 1.3869$ (ref 7, Table I, cubic cell) the critical mass for a singly charged ion is given by

$$m_c = qB^2a^2/8V_{eff}\alpha = 8079 \text{ amu}$$

For calibration errors less than 0.1 ppm, eq 3 would not be useful under the above conditions for masses greater than 11 amu. The large errors indicated in Figure 1 portend the difficulties that will be encountered in the general application of eq 8 over larger mass ranges. However, this does not preclude the application of eq 4 over narrow mass ranges where shifts in frequency due to trapping fields or space charge are nearly independent of mass as in eq 8.

Alternate Calibration Procedure. All previous mass calibration procedures for ICR and FTMS have used mass-frequency relationships which are not appropriate for the cubic analyzer cell, have ignored pressure damping effects, or have employed Taylor series expansions without careful consideration of the errors introduced. In this section we will derive an algebraically exact mass calibration procedure directly from the characteristic equation of the system model. In addition, a consideration of errors due to pressure damping will be included.

To begin, consider the phenomenological equation (*11*)

$$d\mathbf{v}/dt = (q/m)(\mathbf{E} + \mathbf{v} \times \mathbf{B}) - \xi\mathbf{v} \tag{12}$$

together with a Cartesian coordinate system with origin fixed to the center of a cubic analyzer cell (z axis perpendicular to trap plates), a uniform magnetic field of strength B (tesla) parallel to the z axis, and an electric potential of the form (ref 7, eq 3 and 26) at $z = 0$

$$V(x,y,z) = 1/2(V_T) - V_T G_t(x^2 + y^2) - (q\rho G_i/2\epsilon_0)(x^2 + y^2) \tag{13}$$

In eq 12, ξ is the (nonnegative) reduced collision frequency (*11*) of an ion of mass to charge ratio m/q with background neutrals, and $\mathbf{v}$ is the ion velocity. Computing $\mathbf{E}$ from eq 13 and using the definitions 5 and 6, we obtain the system

$$\ddot{x} + \xi\dot{x} - (q/m)2G_T V_{eff}x - \omega_c\dot{y} = 0 \tag{14}$$

$$\ddot{y} + \xi\dot{y} - (q/m)2G_T V_{eff}y + \omega_c\dot{x} = 0 \tag{15}$$

for the equations of motion in the x–y plane. The characteristic equation of the system is

$$\{\lambda^2 + (\xi + \omega_c)\lambda - 2G_T V_{eff}(q/m)\} \times \{\lambda^2 + (\xi - \omega_c)\lambda - 2G_T V_{eff}(q/m)\} = 0 \tag{16}$$

in which λ are the eigenfrequencies of ion motion. A mass calibration law can be computed directly from eq 16 by setting its right-hand factor equal to zero and solving directly for m/q. This is accomplished by first putting

$$\lambda = -\xi_{obsd} + i\omega_{obsd} \tag{17}$$

in which ξ_{obsd} and ω_{obsd} are the observed damping constant and ion resonance frequency, respectively, and $i = -1^{1/2}$. The root of interest is

$$\lambda = (\omega_c/2)\{[-\gamma(m/m_c) + i] - [(\gamma(m/m_c) - i)^2 + m/m_c]^{1/2}\} \tag{18}$$

where

$$\gamma = \xi B/8G_T V_{eff} \tag{19}$$

as derived from the right-hand factor of eq 16 using eq 5–7. Substituting eq 17 into eq 18 and taking the real part

$$\xi^2_{obsd} - \omega^2_{obsd} - \xi_{obsd}\xi = (q/m)(-B\omega_{obsd} + 2G_T V_{eff}) \tag{20}$$

is obtained, from which

$$m/q = \{B/\omega_{obsd} - 2G_T V_{eff}/\omega^2_{obsd}\}/\{1 - \epsilon\} \tag{21}$$

where

$$\epsilon = (\xi_{obsd}/\omega_{obsd})(\xi_{obsd} - \xi)/\omega_{obsd} \tag{22}$$

For the zero pressure case, $\xi = 0$, we obtain a calibration law

$$m/q = B/\omega_{obsd} - 2G_T V_{eff}/\omega^2_{obsd} \tag{23}$$

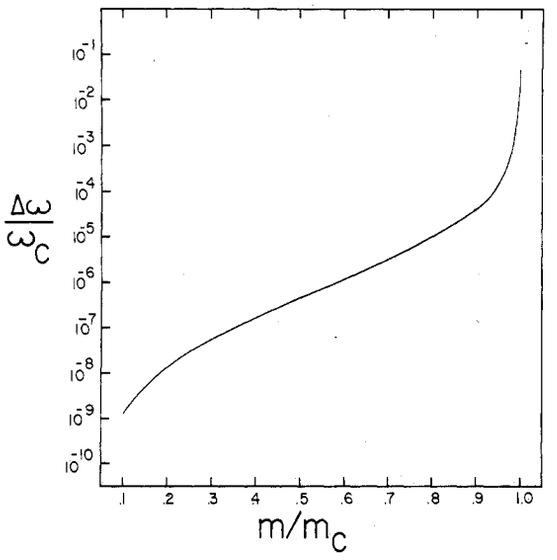

Figure 2. The relative change in observed frequency expected if the pressure is changed from 0 to 10^{-6} torr ($\xi = 0$ to $\xi = 30$) plotted as a function of ion mass (m) normalized to the critical mass (m_c).

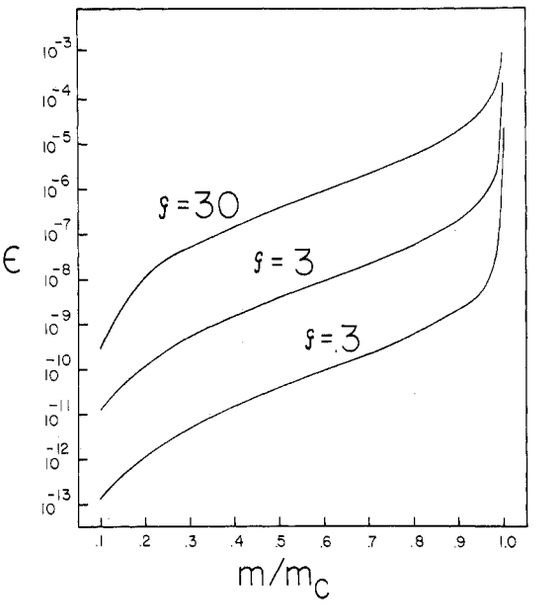

Figure 3. Theoretical relative mass error (ϵ) as a function of m/m_c where m is the ion mass and m_c is the critical ion mass. At a cell pressure of 10^{-6} torr, $\xi \simeq 30$.

However, the pressure is not zero for most practical situations, so care must be exercised in the application of a zero pressure calibration law. It is usual to assume the effect of pressure on the observed resonant frequency, ω_{obsd}, is negligible (7) which, if true, would make the zero pressure calibration unconditionally applicable. Examination of eq 16 indicates that ω_{obsd} depends formally on ξ, and as illustrated in Figure 2, the relative change in frequency between the $\xi = 0$ case and the $\xi = 30$ case is greater than 1×10^{-7} for masses greater than $0.4m_c$. Note the error becomes very large as m/m_c approaches 1. Because there is significant dependence (relative to 0.1 ppm) of the resonant frequency on the reduced collision frequency ξ, particularly at high mass (see eq 16), it is necessary to estimate the mass range for which eq 23 is applicable by considering the size of ϵ.

Before proceeding with a discussion about the size of ϵ, it is worth noting that the right-hand side of eq 22 is mixed in the sense that ω_{obsd} and ξ_{obsd} are experimentally measured parameters while ξ is not. In practice it would be useful to compute ϵ from parameters which can be measured (such as ω_{obsd} or ξ_{obsd}) or inferred from a spectrum; e.g., B and $2G_T V_{eff}$ can be determined by fitting eq 23 to two low-mass peaks where ϵ is known to be very small. To obtain an expression for ϵ suitable for computation, we need the relationship between ξ and ξ_{obsd}. Setting the right hand factor of eq 16 to zero, substituting eq 17, solving for q/m, and taking the imaginary part gives

$$0 = |\lambda|^2(\xi - \xi_{obsd}) + (2G_T V_{eff}\omega_{obsd}/B)(2\xi_{obsd} - \xi) \quad (24)$$

in which $|\lambda|$ is the magnitude of λ. There follows

$$\epsilon = (\xi_{obsd}/\omega_{obsd})^2\alpha/(1 - \alpha) \quad (25)$$

where

$$\alpha = 2G_T V_{eff}\omega_{obsd}/B|\lambda|^2 \quad (26)$$

The quantity ϵ may be viewed, to a first approximation, as the relative error of the zero pressure calibration law, i.e.

$$(m - m_{(\text{zero press.})})/m_{(\text{zero press.})} \cong \epsilon$$

A plot of ϵ at various values of reduced collision frequency ξ at a magnetic field of 1.2 T (see Figure 3) reveals that at a pressure of 10^{-6} torr ($\xi = 30$), errors exceeding 0.1 ppm may be expected from the zero pressure mass calibration law for masses greater than $0.37m_c$, (recall $m_c = 8079$ amu for $B = 1.2$ T and $V_{eff} = 1$ V). At low mass, the pressure damping error varies roughly as the square of ξ. At high mass, on the other hand, pressure damping errors increase rapidly. Nevertheless, under the conditions of the experiment reported in this paper, theoretical error associated with the use of the zero pressure mass calibration law is calculated to be less than 0.01 ppm.

EXPERIMENTAL SECTION

The mass calibration law, eq 23, can be written in the form

$$m = a/f_{obsd} + b/f^2_{obsd} \quad (27)$$

in which the constant a replaces $qB/2\pi$ and the constant b replaces $-2qG_T V_{eff}/(4\pi^2)$. The values of a and b were determined empirically by measuring the frequencies of six reference masses and fitting mass frequency data to the form of eq 27 by means of a least-squares procedure (*12*). By use of the empirical values of a and b and the observed ion frequencies, the theoretical masses of the six ions were computed from eq 27 and compared to the known values.

The six ions employed (m/z 117, 119, 121 and 131, 133, 135) were the major fragments of 1,1,1,2-tetrachloroethane. The observed frequency, ω_{obsd}, of each ion was determined by computing a least-squares parabola through the top five points of each spectral peak and taking the position of the parabola centroid. This process was repeated over a sequence of four mass spectra under a constant set of experimental conditions in order to estimate the precision of frequency (mass) measurements.

Instrumentation. A Varian iron magnet with 0.305 m diameter pole pieces and 0.076 m gap was operated at 1.2 T with current regulation by a Varian Model V-7800 magnet power supply.

Typical FTMS operating conditions were as follows: pressure 3.8×10^{-7} torr; electron beam duration 15 ms; electron beam current 50 nA to 400 nA; delay between beam pulse and rf excitation 1.0 s; mass resolution 30 000 (fwhh); trap voltage 0.34 V. The electron beam was pulsed by toggling the filament bias. No control grid was used, as this would cause electron storage in the ion trap (*14*).

The cubic analyzer cell, first introduced by Comisarow (*15*), was interfaced to a Nicolet Instrument Copr. FTMS 1000 control console. However, home-built interface electronics provided the various potentials to the analyzer cell. In particular, the collector plate was operated at +50 V in order to suppress secondary electron emission from the collector plate surface (*14, 16*). Details of the interface electronics will be discussed in a separate publication.

Number of Ions. The number of ions in the cell was estimated in the following way. The sample was introduced to an indicated pressure of 1×10^{-5} torr with the electron beam operating con-

tinuously and the trap voltage set to +10 V. The charge due to ions diffusing to the transmitter and receiver plates was integrated by using a Keithly 616 digital electrometer for 60 s to give an average ion current. The ratio, σ, or average ion current to indicated collector current was computed using results where the relation is nearly linear, generally for collector currents less than 100 nA. The number of ions was then computed by evaluating the expression

$$\sigma(P_{exptl}/P_{measd})(I_{coll}T_{beam}/e)$$

where P_{exptl} is the indicated partial pressure, P_{measd} is 1×10^{-5} torr, I_{coll} is the collected electron current, T_{beam} is 15 ms, and e is 1.602×10^{-19} C.

Excitation Methods. Two methods of rf excitation were employed. First, a frequency swept sinusoidal excitation ("chirp", 50 kHz to 2 MHz, sweep rate 2.059 kHz/μs was used. Second, an impulse excitation consisting of a nearly critically damped sine wave was applied (*13*). Both excitation wave forms were applied differentially to the transmitter plates of a standard 0.0254 m cubic analyzer cell. Ion image signals were monitored differentially with the receiver plates as has been described previously (*4*).

Signal and Data Processing. The experiment was operated in the mixer mode over the bandwidth 165 kHz to 135 kHz. Between 25 and 10 time domain transients were coadded prior to Fourier analysis. A 32K data buffer was used to store the signal averaged transients. Observation time was approximately three times (*17*) the time constant for exponential decay of ion image signals (*18*, *19*), and no zero filling was employed (*20*).

Single precision floating point computations (30 bit mantissa) were used throughout the study. To ensure that this precision was adequate and to test for ill-conditioned numerical computations (*12*), synthetic spectra with fictitious spectral peaks of precalculated mass were submitted to the mass calibration software (NIC compiler BASIC). Noise traces digitized by the ADC were added to synthetic spectra in order to determine the sensitivity of numerical procedures to random error in the raw data. In all cases, mass measurement accuracy on synthetic spectra was in the range of 2 ppb, which indicated that the numerical procedures, and single precision computations in particular, were sound.

Each spectrum required 30 s to 120 s of time domain signal averaging, so that a set of four successive spectra were acquired in 2–8 min. Over this time period, it was possible for the magnetic field to drift. To help compensate for field drift, it was assumed that the frequency of a given peak would change from one spectrum to the next by the same amount, i.e., that frequency drift was linear with time. For each peak, a least-squares line through a plot of center frequency vs. spectrum number was computed. The slope of this plot indicated the amount of frequency drift which occurred over a set of four trials. Frequency drifts on the order of 0.1 Hz/spectrum to 0.02 Hz/spectrum were observed, from which it was concluded that the magnetic field was sufficiently stable to permit comparison of theory and experiment to 1 ppm or less. Frequency values submitted to the mass calibration software were corrected for the small drifts which were detected.

Protocol. Mass measurement precision and accuracy of some 400 spectra were studied under a variety of experimental conditions. Following exploratory work, systematic studies of mass measurement accuracy and precision as functions of excitation method and the number of ions produced in the analyzer cell were undertaken. Error plots were constructed showing the deviation of calculated masses from the known values, as well as the precision (error bars) of the mass determinations (Figure 4).

RESULTS AND DISCUSSION

At least five relations between the mass-to-charge ratio of ions and the frequencies of their cyclotron modes in ICR and FTMS analyzer cells have been proposed (Table I). The form of each relation depends upon the analyzer cell geometry and upon approximations used in its derivation. Four of these relations apply to analyzer cells with cubic geometry. Two of them, Ledford et al. (*4*) and Francl et al. (*8*) are approximate. The third relation, which we believe to be exact (in spite of approximations used in the derivation) involves the measurement of side band frequencies. Because of the high dynamic range required for such measurements, the method would prove difficult for routine applications.

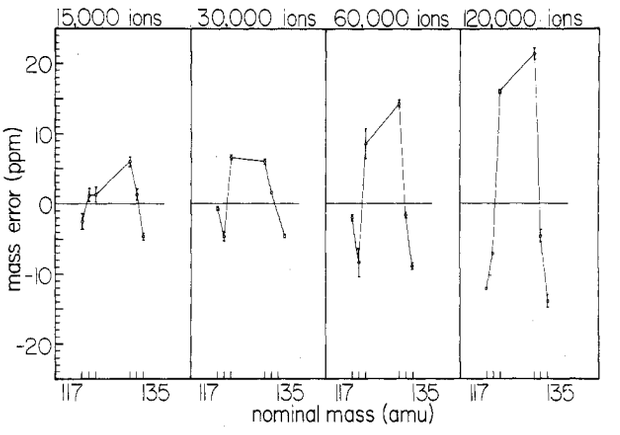

Figure 4. Variation of experimental mass measurement errors with the number of ions formed initially in the cubic cell. Excitation is by chirp.

Table I. Proposed Mass Frequency Relations

$f = a/m$	
$f^2 = a/m^2 + b/m$	Beauchamp–Armstrong (1969) (*22*)
$f^2 = a/m^2 + b/m + c$	Ledford et al. (1980) (*4*)
$f_{sideband} = a/m$	Allemann et al. (1981) (*5*)
$f = a/m + c$	Francl et al. (1983) (*8*)
$m = a/f + b/f^2$	this work

The fourth mass-frequency relation, eq 27 derived in this paper, is algebraically exact in the zero pressure limit. If the premises of the model advanced by Jeffries et al. (*7*) are applicable to the FTMS experiment, the *form* of eq 27 should withstand experimental test. A test of the form of the equation was made by fitting it to experimental data consisting of frequency measurements on a set of ions having known mass-to-charge ratios (see Experimental Section).

One of the essential premises in the derivation of eq 27 is that ion space charge potential should be time invariant and quadratic, as indicated by the third term of eq 13. A test of this linear space charge model can be made by varying the number of ions while holding other parameters constant. If data consisting of frequency measurements on a set of ions having known mass-to-charge ratios are fitted to eq 27, the fit parameter b should change in response to the number of ions. No effect on residual errors should be observed.

Increasing the number of ions from 15 000 to 120 000 produces frequency shifts of 18 Hz, or about 117 ppm, while the range of residual errors changed systematically from 11 ppm to 36 ppm. Apparently, the model accounts for approximately 70% of the space charge effect. Since significant effects on the fit residuals were observed, we conclude that space charge effects are not fully accounted for by the model.

Examination of Figure 4 reveals that changing the number of ions from 15 000 to 30 000 had no effect on the *range* of the fit residuals. This suggests that space charge contributes negligibly, or nearly so, to residual errors obtained when 30 000 ions or less were stored in the cell. The fact that residual errors are systematic (i.e., error bars at the 96% confidence level did not cut the zero error line) with only low numbers of ions in the analyzer cell may indicate nonlinear features in the cell operation not attributable to space charge effects.

Since it appears that the simple linear model derived here is not adequate for describing the mass frequency relation to an accuracy of 0.1 ppm under the conditions of these experiments, the question arises as to what assumptions of the model are violated. One of the underpinnings of the model is the space charge theory of Jeffries et al. (*7*), who have

assumed that a thermal ion cloud in a cubic Penning cell takes the shape of an oblate ellipsoid with a uniform distribution of charge. If excitation were to compromise the shape or uniformity of the space charge distribution, hence the linearity of the space charge electric field, systematic mass measurement errors might be accounted for. Such disturbance of the space charge cloud is probable since, after excitation, the orbital radii of ions are known to be large in comparison to the dimensions of the space charge cloud before excitation.

Systematic mass measurement errors have important implications for elemental composition assignments. For example, the measured mass of the ion m/z 131 would be 130.922 45 ± 0.000 13 amu based on the data in Figure 4. There is no elemental composition consistent with this measurement if the isotopes ^{12}C, ^{13}C, ^{1}H, ^{14}N, ^{16}O, ^{35}Cl, and ^{37}Cl are considered. Clearly systematic errors, even though small, will lead to erroneous elemental composition assignments.

Although systematic errors were obtained, we do not consider the results discouraging. Rather, based on the results, several lines of further work become clear. For example, the method used to excite trapped ions appears to be important. We have found that under conditions similar to those reported here, impulse excitation gives rise to small, *random* mass calibration errors for low numbers of ions in the cell. Correct elemental composition assignments were possible in that case, which will be described in a separate publication. Unfortunately, increasing space charge again produced systematic mass calibration errors. Clearly, effort should be applied toward relieving space charge effects in the FTMS analyzer cell. Two measures that would facilitate this would be the construction of analyzer cells with larger ion holding volume and the development of more sensitive image current amplifiers. The latter would permit spectra to be obtained with fewer ions stored in the analyzer cell. Recently Francl et al. (*8*) have reported mass measurement errors of less than 1 ppm in preliminary studies using a larger (0.0508 m) cubic analyzer cell. Rempel and Ledford (*21*) have introduced a hyperbolic Penning cell which offers the possibility of dispersing the ion charge cloud.

Finally, it should be noted that the simple linear model is in error by only 2–20 ppm. The larger features of the FTMS experiment are correctly described. One of the most striking features of the model is the dominance of the magnetic field. This is reflected in the fact that frequency shifts associated with electric fields in the analyzer cell are small compared to the classical cyclotron frequency, $\omega_c = qB/m$. The relative significance of these electric field effects at a given mass will be reduced in proportion to the square of the magnetic field strength; note the second term of eq 23 diminishes with the square of B. If 20 ppm mass measurement errors are observed at 1.2 T, 0.6 ppm errors should be observed at 7.2 T, an entirely reasonable field strength for a superconducting solenoid magnet.

The developments reported here include a theoretically exact mass calibration law for FTMS, a demonstration of the need for improved experimental methods, and a methodology which can be used to assess improvements. These developments coupled with the use of high field magnets, measures to reduce charge density, and proper excitation methods should produce sufficient agreement between theory and experiment to permit reliable exact mass measurements and assignment of elemental compositions in FTMS.

LITERATURE CITED

(1) Comisarow, M. B.; Marshall, A. G. *Chem. Phys. Lett.* **1974**, *25*, 282–283.
(2) Ledford, E. B., Jr.; McIver, R. T., Jr. *Int. J. Mass Spectrom. Ion Proc.* **1976**, *22*, 399–406.
(3) Comisarow, M. B. "Fourier, Hadamard, and Hilbert Transforms in Chemistry"; Marshall, A. G., Ed.; Plenum: 1982.
(4) Ledford, E. B., Jr.; Ghaderi, Sahba; White, R. L.; Spencer, R. B.; Kulkarni, P. S.; Wilkins, C. L.; Gross, M. L. *Anal. Chem.* **1980**, *52*, 463–468.
(5) Allemann, M.; Kellerhals, Hp.; Wanczek, K. P. *Chem. Phys. Lett.* **1981**, *84*, 547–551.
(6) White, R. L.; Onyiriuka, C.; Wilkins, C. L. *Anal. Chem.* **1983**, *55*, 339–343.
(7) Jeffries, J. B.; Barlow, S. E.; Dunn, G. H. *Int. J. Mass Spectrom. Ion Proc.* **1983**, *54*, 169–187.
(8) Francl, T.; Sherman, M. G.; Hunter, R. L.; Locke, M. J.; Bowers, W. D.; McIver, R. T., Jr. *Int. J. Mass Spectrom. Ion Proc.* **1983**, *54*, 189–199.
(9) Byrne, J.; Farago, P. S. *Proc. Phys. Soc.* **1965**, *86*, 801–815.
(10) Davidson, R. C. "Theory of Non-neutral Plasma"; W. H. Benjamin: New York, 1979.
(11) Beauchamp, J. L. *J. Chem. Phys.* **1966**, *46*, 1231–1243.
(12) Ralston, A.; Rabinowitz, P. "A First Course in Numerical Analysis"; McGraw-Hill: New York, 1978.
(13) Rempel, D. L. Presented at the Thirty-first Annual Conference on Mass Spectrometry and Allied Topics, Boston, MA, May 9–13, 1983; pp 398–399.
(14) Ledford, E. B., Jr.; Rempel, D. L.; Gross, M. L. *Int. J. Mass Spectrom. Ion Proc.* **1984**, *55*, 143–154.
(15) Comisarow, M. B. *Int. J. Mass Spectrom. Ion Phys.* **1981**, *37*, 251–257.
(16) Heppner, R. A.; Walls, F. L.; Armstrong, N. T.; Dunn, G. H. *Phys. Rev. A* **1976**, *13*, 1000–1011.
(17) Marshall, A. G. *Anal. Chem.* **1979**, *51*, 1710–1714.
(18) Shockley, W. *J. Appl. Phys.* **1938**, *9*, 635.
(19) Comisarow, M. B. *J. Chem. Phys.* **1978**, *69*, 4094–4104
(20) Giancaspro, C.; Comisarow, M. B., *Appl. Spectrosc.* **1983**, *37*, 153–165.
(21) Ledford, E. B., Jr.; Rempel, D. L. Presented at the 31st Annual Meeting of the American Society for Mass Spectrometry, Boston, MA, 1983; pp 402–403.
(22) Beauchamp, J. L.; Armstrong, J. T. *Rev. Sci. Instrum.* **1969**, *40*, 123.

RECEIVED for review September 9, 1983. Resubmitted May 7, 1984. Accepted July 16, 1984. This work was supported by the National Science Foundation (Grant No. CHE-8018245) and the National Institutes of Health (Grant No. 2-8423576).